

Rose-Hulman Institute of Technology

Rose-Hulman Scholar

Graduate Theses - Physics and Optical
Engineering

Graduate Theses

8-2023

Design of a Resonant Optical Cavity for Imaging Magneto-Optically Active Thin Film Samples

Cody Robert Brelage

Rose-Hulman Institute of Technology

Follow this and additional works at: https://scholar.rose-hulman.edu/optics_grad_theses



Part of the [Optics Commons](#)

Recommended Citation

Brelage, Cody Robert, "Design of a Resonant Optical Cavity for Imaging Magneto-Optically Active Thin Film Samples" (2023). *Graduate Theses - Physics and Optical Engineering*. 31.

https://scholar.rose-hulman.edu/optics_grad_theses/31

This Thesis is brought to you for free and open access by the Graduate Theses at Rose-Hulman Scholar. It has been accepted for inclusion in Graduate Theses - Physics and Optical Engineering by an authorized administrator of Rose-Hulman Scholar. For more information, please contact ligget@rose-hulman.edu.

**Design of a Resonant Optical Cavity for Imaging Magneto-Optically Active Thin Film
Samples**

A Thesis

Submitted to the Faculty

of

Rose-Hulman Institute of Technology

by

Cody Robert Brelage

In Partial Fulfillment of the Requirements for the Degree

of

Master of Science in Optical Engineering

August 2023

© 2023 Cody Robert Brelage



ROSE-HULMAN INSTITUTE OF TECHNOLOGY

Final Examination Report

Name _____

Graduate Major _____

Thesis Title _____

DATE OF EXAM:

EXAMINATION COMMITTEE:

| Thesis Advisory Committee | Department |
|---------------------------|------------|
| Thesis Advisor: | |
| | |
| | |
| | |
| | |

PASSED _____

FAILED _____

ABSTRACT

Brelage, Cody Robert

M.S.O.E.

Rose-Hulman Institute of Technology

August 2023

Design of a Resonant Optical Cavity for Imaging Magneto-Optically Active Thin Film Samples

Thesis Advisor: Dr. Azer Reza

This document describes the design and fabrication of an optical resonator system to investigate magneto-optic properties of thin film samples. This system uses an open-air optical resonator to enable photons to make multiple passes through each thin film and thus increase the magnitude of the Faraday rotation that each sample imposes onto the light that exits the system. This system promises many future experiments to study the magneto-optic properties of thin film and nano-particle samples. Using an optical resonator to enhance Faraday rotation should enable an improved signal-to-noise ratio in taking measurements and images with a photodetector.

Key Words: optical engineering, magneto-optics, Faraday effect, resonator, cavity

DEDICATION

To my loving and supporting family and friends who have been there for me throughout it all.

ACKNOWLEDGMENTS

This project would not have been possible without the help of Elizabeth Canon, who aided with the initial phases of design. Additionally, I would like to acknowledge Dr. Azer Reza and Dr. Maarij Syed, without whose passion and expertise this project would never have occurred.

TABLE OF CONTENTS

| | |
|------------------------------------|-------------|
| LIST OF FIGURES | iii |
| LIST OF ABBREVIATIONS | iv |
| LIST OF SYMBOLS..... | vi |
| GLOSSARY | viii |
| 1. INTRODUCTION | 1 |
| 2. BACKGROUND | 3 |
| 3. DESIGN..... | 10 |
| 4. FABRICATION | 17 |
| 5. RESULTS | 27 |
| 6. DISCUSSION..... | 31 |
| 7. LIMITATIONS | 33 |
| 8. CONCLUSIONS..... | 35 |
| 9. FUTURE WORK..... | 36 |
| LIST OF REFERENCES | 37 |

LIST OF FIGURES

| | |
|--|----|
| Figure 1: Concentric and Folded Concentric Resonator Geometries | 5 |
| Figure 2: Number of Round Trips Inside the Cavity Due to Partial Mirror Reflectivity..... | 6 |
| Figure 3: Optical Geometry of a Beam Expander | 9 |
| Figure 4: Ray-based Design for a Resonant Optical Cavity | 12 |
| Figure 5: Progression of Polarization as Light Passes through the System..... | 15 |
| Figure 6: Complete Fabricated Optical System | 17 |
| Figure 7: Schematic Drawing of Complete Fabricated Optical System | 18 |
| Figure 8: Schematic Depiction of Autocollimation Setup | 24 |
| Figure 9: Schematic Configuration for Measurement of Light Incident on the Partial Mirror | 27 |
| Figure 10: Schematic Configuration for Measurement of Light Entering the Cavity | 28 |
| Figure 11: Schematic Configuration for Measurement of Light in a Non-Resonating System.... | 29 |
| Figure 12: Schematic Configuration for the Measurement of Light in a Resonating System..... | 29 |

LIST OF ABBREVIATIONS

DPSS: Diode-pumped solid state

Nd:YVO₄: Neodymium Doped Yttrium Orthovanadate

KTP: Potassium Titanyl Phosphate (KTiOPO₄)

FWHM: full width at half max

FSR: free spectral range

MO: microscope objective

PH: pinhole

AP: aperture (this is followed by a number)

L: lens (this is followed by a number)

M: mirror (this is followed by a number)

P: polarizer

GTP: Glan-Thompson polarizer

HWP: half-wave plate

PBS: polarizing beam splitter

FR: Faraday rotator

COTS: commercial off the shelf

Q-factor: quality factor

SNR: signal-to-noise ratio

LIST OF SYMBOLS

θ : Faraday rotation introduced to polarization

V: Verdet constant

B: magnetic field

d: distance traveled within a sample in a magnetic field

ρ : radius of curvature

L_C : length of the cavity

N: average number of round trips a photon makes in a cavity

R: reflectivity of a surface

c: the speed of light in a vacuum

$\bar{\tau}$: average photon lifetime in the cavity

\mathcal{F} : finesse

n: refractive index inside the cavity

ν_m : resonating frequency of the cavity

$\Delta\nu$: FSR of the cavity

Q: quality factor

W: width of the beam

OPL: optical path length.

F: focal length

mm: millimeter

MHz: megahertz

nm: nanometer

ns: nanosecond

mW: milliwatt

μ W: microwatt

X: distance along the direction of the optical axis

α : full-angle beam divergence

ϵ : permittivity of the medium inside the cavity

GLOSSARY

Finesse: the ratio between FSR and FWHM, a measure of the resolving power of a cavity (Svelto)

Faraday effect: the rotation of the polarization of light passing through a sample subjected to a magnetic field (Faraday)

Quality factor: the ratio between the resonating frequency of a cavity and its FWHM (Svelto)

1. INTRODUCTION

The Faraday effect is a well-known magneto-optic phenomenon that finds much use optics and physics. The effect manifests itself in the rotation of the plane of light polarization when a magnetic field is present inside a magneto-optic material. One of the most common uses of this phenomenon is in the creation of optical isolators, which allows light to pass through in one direction, similar to a diode in electric circuits while preventing the unwanted back reflections from entering back into the source of the system, which is often a laser, to maintain the source's stability and prevent unwanted interference.

The Faraday effect often also finds use in characterizing new and existing materials. In 2019, Syed, Monarch, Li, and Fried used an AC-modulated magnetic field to induce Faraday rotation in samples, including glass coated in transparent conducting oxide films to determine the Verdet constants of such materials. In this experiment, the researchers used only a single pass of light through each sample in their investigation, which typically showed samples introducing around a tenth of an arc minute of rotation (Syed, Monarch, and Li).

Similarly, other research that has been conducted regarding methods by which to measure the Verdet constant of magneto-optic materials focuses on single-pass effects of these magneto-optic materials given a controlled AC magnetic field and the use of a lock-in amplifier when seeking to reduce the amount of power required by the system for relevant measurements to be collected (Jo, Kim, and Hwangbo).

In chemistry, the measurement of Faraday rotation enhances established methods of sensing trace radicals, which is an important point of interest to a “broad range of fields, including chemistry, medicine, and combustion dynamics” (Gianella, Press, and Manfred). By introducing the Faraday effect into the established absorption technique known as cavity ring-down spectroscopy, Gianella, Press, Manfred, Norman, Islam, and Ritchie showed that they were able to gather additional information about the radical species that they were studying while also increasing the sensitivity of their measurements by a factor of five and allowing for the measurements of faint Faraday effects.

Using an optical resonator cavity, our design should allow for enhanced sensitivity and signal-to-noise ratio in the study and characterization of thin film and nano-particle samples, which are difficult to study and characterize due to their extremely thin profile. The optical resonator capitalizes on the non-reciprocal nature of Faraday rotation to enhance and magnify the polarization rotation induced by thin film samples on light exiting the resonant cavity. By using a lock-in amplified and AC modulated magnetic field, this design will build on existing setups to allow for an enhanced signal in samples with weak magneto-optic properties while maintaining a low level of noise.

This document describes the design, fabrication, and alignment of this system that uses an optical resonant cavity to enhance the Faraday effect applied by a sample, thus allowing for easier study of magneto-optical properties in thin-films and nano-particle samples.

2. BACKGROUND

Two major topics are to be discussed in this section, the Faraday effect and optical resonators, as these are the two major concepts to be used in designing an optical system for this application.

The Faraday effect is a well-known phenomenon discovered by Michael Faraday (Faraday). It causes the polarization of light to be rotated when passing through a material under the influence of a magnetic field along the direction of light propagation (Van Baak). The angle by which the polarization is rotated is determined by the equation,

$$\theta = V B d \quad 1$$

where θ represents the angle of rotation caused in the polarization, the Faraday rotation, V is the Verdet constant, B is the magnetic field in the direction of the light propagation, and d is the distance traveled through the sample in the magnetic field (Valev, Wouters, and Verbiest). While much more information about Faraday rotation and its uses has been discovered, the scope of this project would be exceeded by a deeper study of it. The rotation of polarization due to the Faraday effect is in the same direction no matter the direction that light passes through the Faraday rotator because magnetic field is a direction-dependent vector. The vector nature of the magnetic field is factored into the equation by the specification that B is the magnetic field in the direction of light propagation rather than the magnitude of the magnetic field. That is to say, if the light is reflected and passes through the Faraday rotator again, but traveling in the opposite direction this time, the light that exits the Faraday rotator after its second pass will have twice the rotation from its starting

state than it does through a single pass through the sample. All this is to say that Faraday rotation is a non-reciprocal phenomenon, as it does not reverse itself upon passing through the rotator again in the opposite direction, as is true for such a device as a half-wave plate.

Optical resonators have seen many uses, but potentially the most well-known variation of an optical resonator is the Fabry-Perot resonator, which uses two plane mirrors set parallel to one another. However, the design we are using is a concentric resonator or rather a folded concentric resonator. In a concentric resonator configuration, the length of the resonator cavity, L is equal to the sum of the radius of curvature of the mirrors used to create it, as seen in the following equation,

$$\rho_A + \rho_B = L \quad 2$$

where ρ_A is the radius of curvature of the first mirror and ρ_B is the radius of curvature of the second mirror. In the case of a folded concentric resonator, a flat mirror is inserted into the center of what the cavity would normally be, and as such, the length of the cavity becomes

$$\rho_B = L_C \quad 3$$

due to the fact that a flat mirror has no radius of curvature, and the cavity is effectively turned back onto itself, at the halfway point as long as mirror ‘A’ is considered to be the flat mirror and mirror ‘B’ is considered to be the curved mirror (Svelto; Yariv and Yeh). The comparison of a concentric cavity and a folded concentric resonator geometry can be seen in Fig. 1.

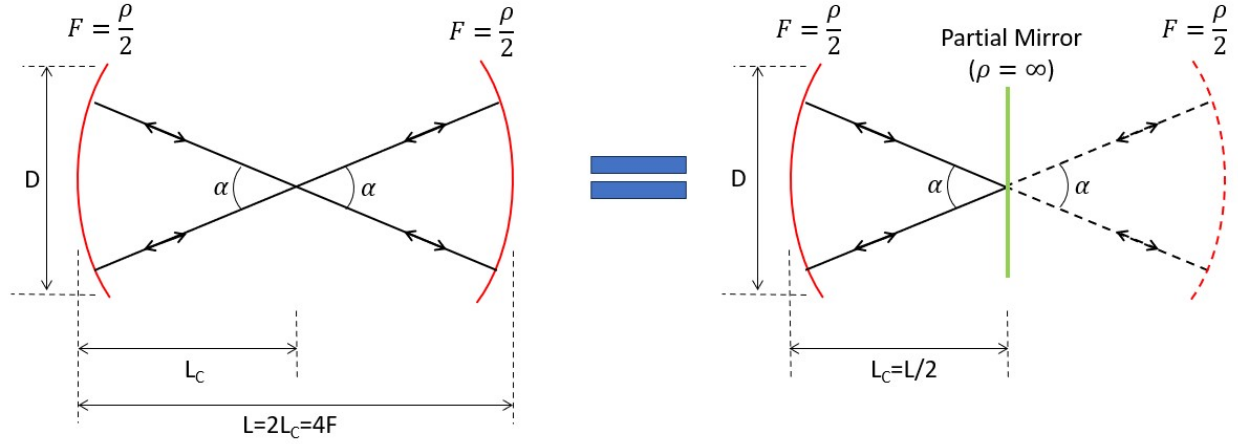


Figure 1: Concentric and Folded Concentric Resonator Geometries

When designing an optical resonator, it is imperative that one also considers the reflectivity of the mirrors being used to construct it, as this affects the number of passes that each photon makes through the cavity before being released and its related photon lifetime (the average amount of time that each photon exists within the cavity before exiting). The average number of round trips that a photon makes inside a resonant cavity with only one mirror that is partially transmitting can be described by the equation

$$N = \frac{1}{1 - R_A} \quad 4$$

where R_A is the reflectivity of the partial mirror, mirror 'A' (Reza, Syed, and Brelage). A graph of the number of roundtrips with respect to R_A is shown in Fig. 2.

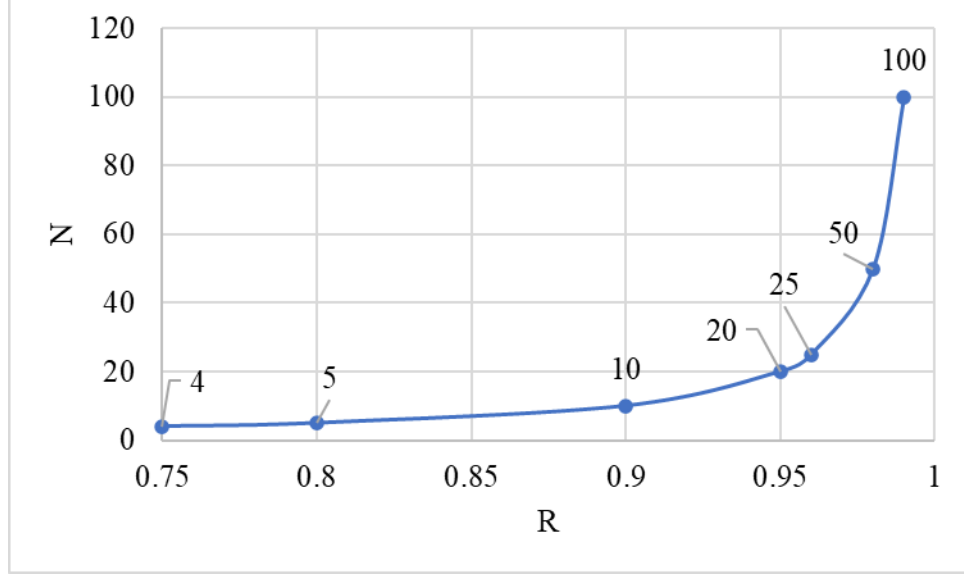


Figure 2: Number of Round Trips Inside the Cavity Due to Partial Mirror Reflectivity

R_A values of 0.96, 0.98, and 0.99 give 25, 50, and 100 round trips, respectively.

Following this, the average lifetime $\bar{\tau}$ can be calculated as

$$\bar{\tau} = \frac{2L_c N}{c} \quad 5$$

where c is the speed of light in a vacuum (Svelto).

When designing an optical cavity, it is also of interest to see what the finesse of your cavity is, finesse being the ratio between the free-spectral range, FSR, and the full-width at half maximum, FWHM, of any of the resonant peaks of the resonating modes. The finesse is a measure of the resolving ability of a cavity, and as such, a high finesse is desirable. It can be calculated with knowledge of the reflectivity of the mirrors to be used in building the system. The equation for this is given as

$$\mathcal{F} = \frac{\pi(R_A R_B)^{\frac{1}{4}}}{1 - (R_A R_B)^{\frac{1}{2}}}. \quad 6$$

The value for finesse is usually much greater than one, which is what one would hope to see (Reza, Syed, and Brelage; Svelto; Yariv and Yeh).

Only specific frequencies can resonate within an optical cavity, and the resonating frequencies can be calculated using the following equation

$$\nu_m = \frac{mc}{nL_C} \quad 7$$

where m is an integer and n is the refractive index within the cavity, and the frequency difference between two successive resonant modes can be found as

$$\Delta\nu = \frac{c}{2nL_C}, \quad 8$$

which is the FSR of the cavity. Dividing the FSR by the finesse will give you the value of FWHM, which gives information about the width of each peak (Peatross and Ware; Kogelnik and Li; Yariv and Yeh).

Using this information, we can also calculate the quality factor, Q-factor, of the resonant cavity. The Q-factor is the relationship between the resonance frequency and the linewidth, or FWHM frequency as seen in

$$Q = \frac{\nu_m}{\Delta\nu_c} \quad 9$$

(Kogelnik and Li; Yariv and Yeh). If this eq. 9 is then translated to a form that makes more sense given the parameters that we know and have used to find the finesse,

$$Q = \frac{1}{4} \omega \epsilon \eta L \frac{(1 - R_A)^2 (R_B)}{[1 - \sqrt{R_A R_B}]^2} \quad 10$$

becomes the version of the equation for the Q-factor that we can use for consideration.

Reviewing equations 6, 8, and 10, we can better understand the relationship between finesse, FSR, and Q-factor for a resonant cavity. As stated previously, finesse is the ratio between FSR and FWHM. Thus, these two values are proportional, so if one gets larger, the other does as well. The Q-factor is also proportional to finesse by the following relationship

$$Q = \mathcal{F} \left(\frac{\nu_m}{\Delta\nu} \right), \quad 11$$

which indicates that it is also inversely proportional to the FSR (Svelto). In this case this indicates the Q-factor is impacted more by the FWHM of the cavity and its reflection in the finesse value rather than the FSR value.

The beam's diameter is important so that the entirety of the light is captured on the second mirror, the curved mirror, of the resonator. To change the size of a beam, two lenses can be used in tandem with one another in a configuration that is known as a beam expander, which can be seen in Fig. 3. When collimated light is put into a beam expander whose lenses are the sum of their focal lengths apart, the beam that exits will still be collimated, but the diameter of the beam will be scaled by a factor of their focal lengths according to the following equation,

$$W_{out} = \left(\frac{F_2}{F_1} \right) W_{in} \quad 12$$

where W is the width of the beam, and F is the focal length of each lens. F_1 being in reference to the first lens, and F_2 in reference to the second lens, respectively (Peatross and Ware).

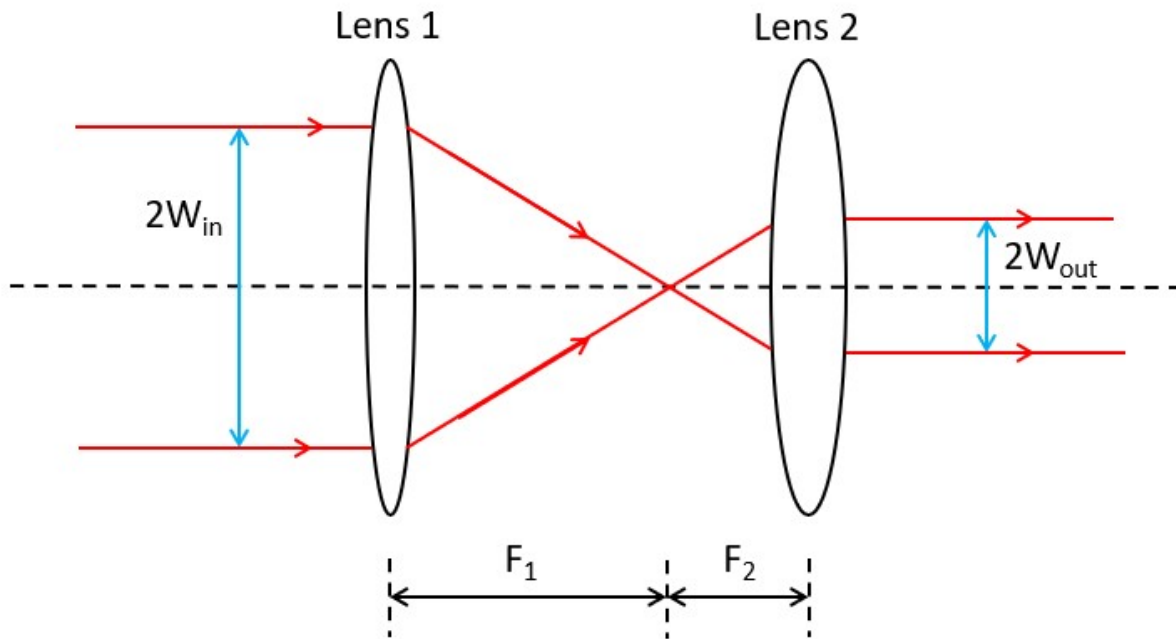


Figure 3: Optical Geometry of a Beam Expander

When a sample is introduced into the path of light, it changes the path that the light travels, even if it doesn't change the shape of the beam or its wavefront. As this design is intended for use with a sample that has two, flat, parallel surfaces introduced into the cavity, it is important to be aware of this phenomenon. The optical path length (OPL) of light passing through this sample will follow a simple and well-known rule, as seen in the equation

$$OPL = nd. \quad 13$$

Equation 13 tells us that if we use a microscope slide, which is about 1mm thick and generally has a refractive index of around 1.5, the OPL through this material is 1.5mm, as d represents the thickness of the material in this equation. If the optical path length through a 1mm thick material is 1.5mm, then the cavity will need to be shortened by 0.5mm to return to the original cavity length and continue resonating with the sample in place.

3. DESIGN

To design a system that can be used for our application, we must first be very clear on what we hope to achieve with it so that we can make decisions accordingly. The long-term goal for this system is to measure the effect of Faraday rotation induced upon light passing through a thin film. Due to Faraday rotation being reliant upon the thickness of a sample and the magnetic field being applied to it, a design must be created that can not only apply a magnetic field, but it must also be able to effectively increase the thickness of the sample that the light passes through. Additionally, this system should be able to be used for the evaluation of multiple different samples.

The first of those two considerations is simple to account for. We could attempt to place magnets near the sample or use a solenoid around the sample to generate a magnetic field. Of these options, the only one that works is the solenoid, as we want the magnetic field direction to match the direction of the optic axis. Additionally, we need to be able to control the strength of the magnetic field so that we can assess the Faraday rotation induced upon the sample at multiple different magnetic field strengths.

The second consideration also has a relatively simple solution, but it requires a lot more precision to implement. One way to effectively increase the thickness of a sample is to increase the number of passes that the light makes through the sample. To increase the number of passes that the photons make through the sample, the path that the light takes must fold back on itself and resonate similarly to what occurs in a laser. Due to the non-reciprocal nature of Faraday rotation, it is reasonable to pass through the sample multiple times in both directions along the optical axis.

Therefore, rather than trying to make the thin film itself thicker, which would require very precise cleanroom practices and many places to introduce error, we decided to create an optical resonator.

The third major consideration that was stated in this section's first paragraph serves to complicate the matter, as it means that we would need to have easy access to the inside of a resonant cavity, which is a very carefully and precisely aligned system. Not only that, but it means that there would need to be a means of precisely changing the length of the cavity because the introduction of any components into the cavity changes the optical path length within the cavity, which must be very precisely controlled to be able to resonate.

Given that we would be creating this fixture on an optical table, we have a limited length to work with to build our system, and we want to make sure that whatever we build is a manageable size that can also fit a sample and a solenoid between the mirrors that make up the cavity. Not only that, but we need to be able to fit an input laser source and other optical components for the system onto the table as well to control the shape and polarization of the wavefront that enters into the resonant cavity.

The final, unstated design condition is that we would like to use as many components as possible already accessible to us at Rose-Hulman. If a component could not be found to fit our setup, we would want to stick with purchasing commercially available COTS optical components. With all of these considerations in mind, the process of designing the system could begin.

For our system, we started to come up with some basic metrics and values so that we could start on the design. We began by thinking about the amount of space that we wanted the cavity to take up, and so a cavity length in the range of one to two feet was mentioned, as it would give plenty of space for the Helmholtz coil and sample within the cavity without being too large. We

also know that the longer a cavity is, the more frequencies can resonate within it as its FSR shrinks, so we wanted to keep the cavity from getting too large. With this in mind, the general optical setup seen in Fig. 4 was conceived.

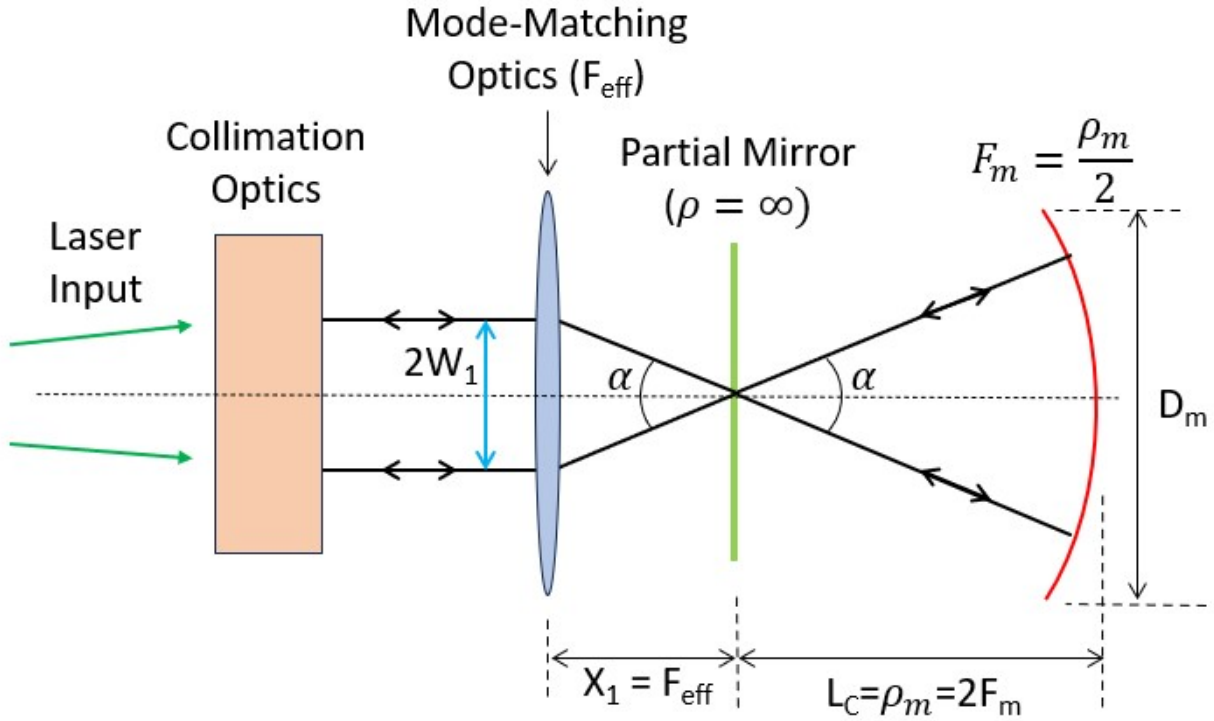


Figure 4: Ray-based Design for a Resonant Optical Cavity

Based on this assessment and common focal lengths of mirrors for COTS components, it was decided that a mirror with a focal length of 250mm would be our target for the curved mirror. With a focal length of 250mm, the mirror has a radius of curvature of 500mm, and thus by eq. 3, our cavity length would need to be 500mm. At a length of 500mm, the cavity would have a FSR of 300MHz (see eq. 8). At this point we also needed to check what the resonant frequencies of the cavity would be, so we used eq. 7, and the general relationship between frequencies and wavelengths to find that when $m = 939,850$, the cavity resonates for our desired wavelength of 532nm. When a sample is inserted into the cavity, the cavity length must be adjusted to compensate

for the additional optical thickness such that the optical path length within the cavity remains the same; hence the FSR remains the same. By modifying eq. 8, we obtain

$$\Delta\nu = \frac{c}{2(n_1(L_c - OPL) + OPL)}, \quad 14$$

where n_1 is the index of refraction of the part of the cavity that is not taken up by the sample. In the case of our experiment, we can expect the FSR to stay the same at 300MHz so long as we assume that the index of refraction of air is 1.

With this confirmed that our chosen wavelength will resonate in a cavity of 500mm length, we began to look at partial mirrors. Based on the reflectivity of the available mirrors, we began to look into an 80% reflective mirror ($R=0.8$), as it was available COTS. We chose to use a mirror with a slightly lower reflectivity as our partial mirror because though a higher reflectivity would allow for a greater number of passes through the sample, it would also limit the amount of light that is able to enter the cavity and pass through the sample, and we desired to get as much light as possible into the cavity to improve our SNR since the signal from the cavity would be detected alongside the light initially reflected off of the partial mirror. Using eq. 4, we found that a mirror of this reflectivity would allow an average photon to complete 5 round trips in the resonator before exiting. This means the light would pass through the sample a total of ten times. Additionally, using eq. 5 we can find that an average photon would spend 16.67ns in the cavity.

Given this information, it is important we figure out what finesse we can expect to see from our cavity, so given that we are using a fully reflective mirror and a mirror that is 80% reflective, we can use eq. 6 to find that the finesse of our system is 28.1, which is much greater than one, like we desired it to be. We can also determine the intensity gain that we should see from the cavity using the following equation,

$$G = \left[\frac{\sin(2N\theta)}{\sin(\theta)} \right]^2. \quad 15$$

By using the number of round-trips that each photon makes on average, we can determine that our intensity gain from eq. 15 would be $G = \left[\frac{\sin(10\theta)}{\sin(\theta)} \right]^2$ (Reza, Syed, and Brelage). As stated in the introduction, thin film samples often introduce around a tenth of an arc minute in rotation, so this gain should make a significant improvement regarding accurate and useful measurements of Faraday rotation.

With decisions made about the cavity, it comes time to select the components for the rest of the system. Another necessary component is the mode-matching lens which will be placed in front of the flat partial mirror. Knowing that the minimum spot of the beam at the flat partial mirror is a necessity for the beam to resonate and be stable, the distance between the mode-matching optics and the partial mirror would need to be equal to the F_{eff} of the mode-matching optics, as can be seen in Fig. 4. To find the focal length of the mode-matching optics, we can take a look at beam widths and the relationship

$$F_{\text{eff}} = \frac{2W_1 L_C}{D_m}. \quad 16$$

To simplify things, we decided to look at a 2:1 relationship between the beam width at the mode-matching optics, $2W_1$, and the width of the beam at the mirror, D_m , which leads to an F_{eff} that is half of the length of the cavity. Thus, we choose to use a focal length that could be found easily as COTS. We chose to use a focal length of 250mm, which matches all our calculations for cavity length and the relationship set forth in eq. 16. Due to this focal length, the lens would need to be placed exactly 250 mm away from the flat mirror to have the reflective side of the mirror exactly at its focal point.

The rest of the system needed to be designed with polarization and beam control in mind. Thus, it was decided that given the materials that we had access to, we would be using a spatial filter to clean the wavefront of the beam output from the laser diode, a Glan-Thompson polarizer to achieve linear polarization, and a half-wave plate to control the direction of this linear polarization. These components would need to be in the first half of the setup, as they deal almost solely with beam conditioning and preparation for the cavity. After that, a polarizing beam-splitter would be used to change the direction of the output beam while letting the maximum amount of light into the system. To get the maximum amount of light back out of the cavity, a 45° Faraday rotator needed to be introduced on the back half of the system so that between the two passes, the polarization would undergo 90° of rotation. Thus all be reflected instead of transmitted through the system. The polarization change as the light passes through the system can be visualized in Fig. 5. The components shown in this figure are named in accordance with Figs. 6 and 7, and the only components that are shown are the first ones that change the polarization of the light at each point through the setup.

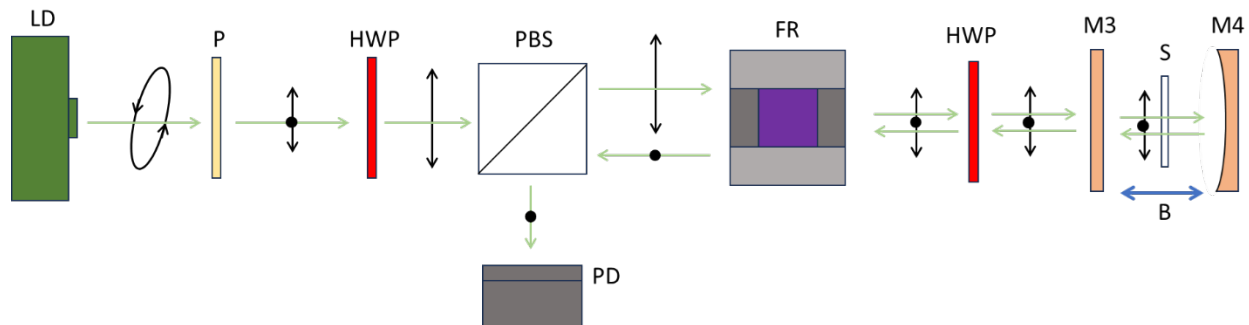


Figure 5: Progression of Polarization as Light Passes through the System

In order to have a greater degree of control over the system, incorporating additional degrees of freedom and finer control of positioning became necessary. To meet this challenge, it was decided that a computer-controlled linear actuator would be used for the curved mirror to

allow more precise control of its position while minimizing human error. At all possible points with the cavity mirrors, it was decided that motorized stages should be used to increase the precision with which each component could be moved.

Throughout the fabrication process, many speedbumps were encountered, and components needed to be inserted into the system. Thus, eq. 12 saw use when the aperture of the Faraday rotator was much smaller than expected. Choices made to change the design during the fabrication process will be outlined in greater detail within that section.

4. FABRICATION

A major component of this project was constructing the system that we had designed through mathematical analysis and design. The fabrication of this design will be discussed on a component-by-component basis, along with a short discussion about these choices. The final fabricated system, pictured in Fig. 6, will guide this discussion alongside the system drawing found in Fig. 7.

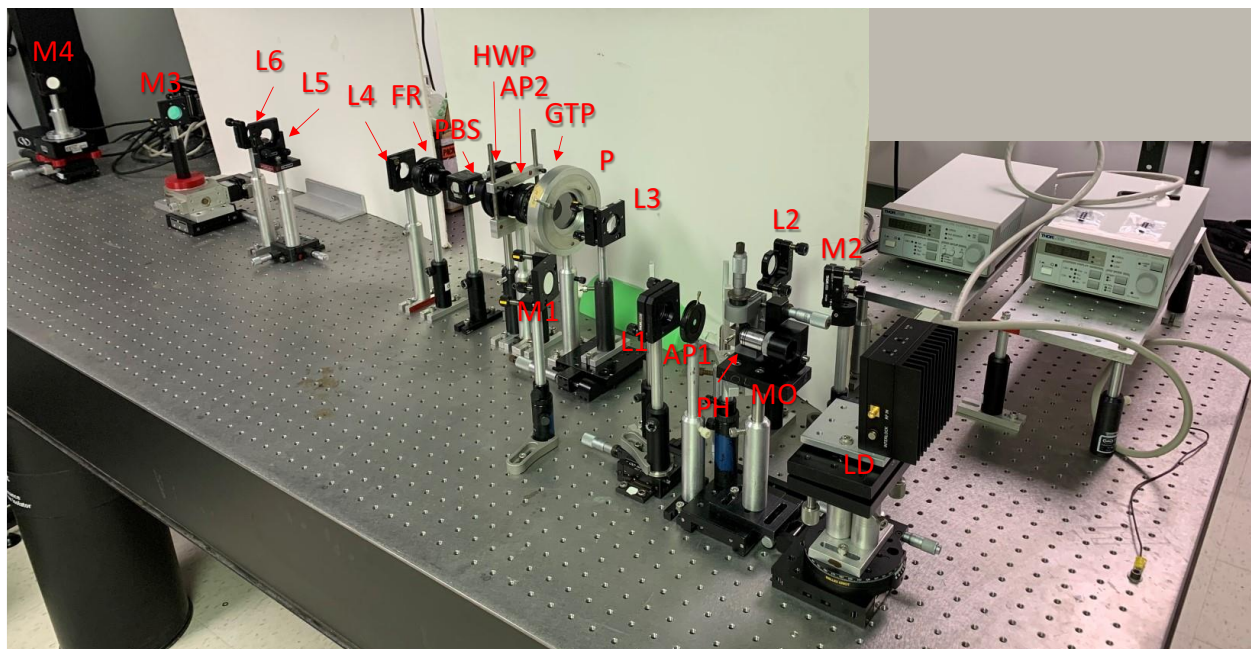


Figure 6: Complete Fabricated Optical System

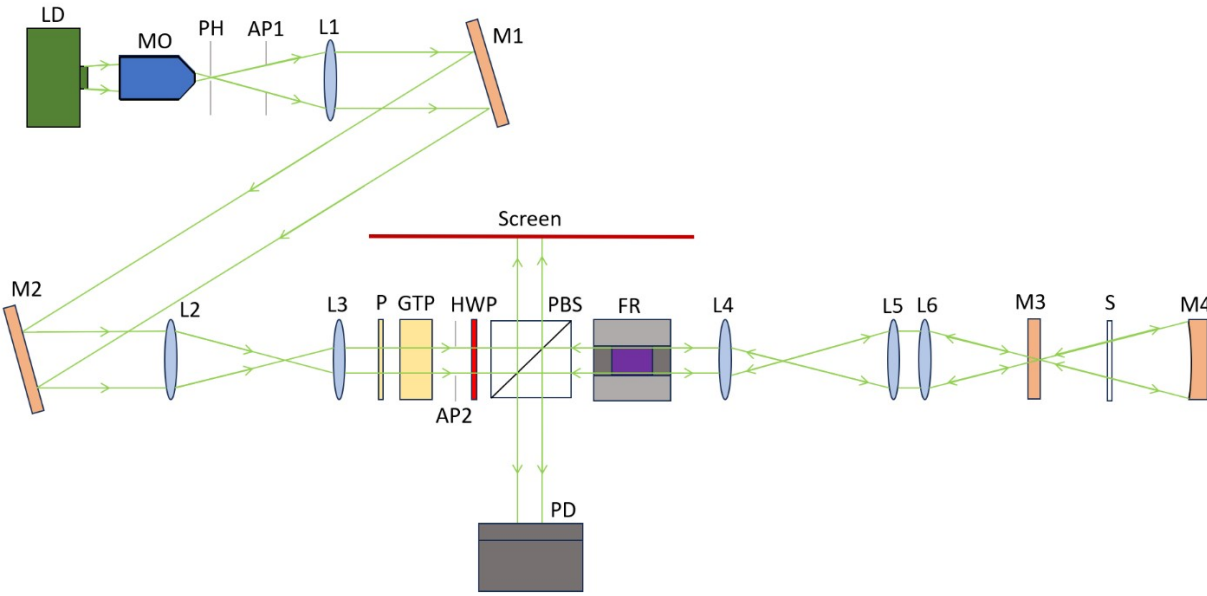


Figure 7: Schematic Drawing of Complete Fabricated Optical System

As with any optical build, a good place to start is with the light source. The 40mW 532nm laser diode (Thorlabs DJ532-40) and its thermo-electrically cooled TCLDM9 Thorlabs mount were mounted on a tip/tilt stage to maximize the degrees of freedom available for alignment. In both system figures (Fig. 6 and Fig. 7), the component labeled LD represents the source, as it stands for laser diode. In the case of the specific laser diode source that we used, it is more specifically a Diode-Pumped Solid State (DPSS) laser, which is made by a combination of Nd:YVO₄ and KTP crystals pumped by an 808nm laser diode. These can be used the same as a typical semiconductor LD but offer a much smaller beam divergence and output light with nearly linear polarization.

The output of this LD was then passed into a microscope objective, MO in Fig. 6 and Fig. 7. This microscope objective was then focused onto a pinhole (PH) 5 μ m in diameter. Combining of these two components is a standard practice in optics for use as a spatial filter. The light passing

through these components was then passed through an aperture, AP1, to eliminate any extra stray light that may make its way into the system.

The next component in the design is L1, or the first lens in the setup. This lens is used as our collimation lens. For proper collimation, the lens must be placed a distance away from the pinhole equal to its focal length. As L1 is a 100mm focal length lens, it was placed 100mm from the pinhole end of the spatial filter. Because it is being used for collimation, it is of utmost importance that the lens is properly placed, so it was mounted in a tip-tilt mount on top of a linear translation stage to allow for as many degrees of freedom as possible for reaching the proper position for collimation. To check for collimation of the light after passing through this lens, a shear plate was used to observe the fringe pattern caused by light incident upon it and ensure that the fringes appeared horizontal, indicating proper collimation.

Despite our best efforts, the mount of the LD components did not offer enough adjustment range to fully make the optic axis of the output beam parallel to the top of the table. To correct these errors, flat mirrors M1 and M2 were added to the system in tip/tilt mounts. These were also adjusted after their initial installation to give a greater amount of linear table space so that the components could all be properly spaced from one another without needing more space than the table would allow.

The following two components, L2 and L3, will be viewed as a group, since they are used to fulfill a single function. L2 is a 200mm focal length lens, while L3 is a 40mm focal length lens. The combination of any two lenses can allow for the recollimation of the light with a different beam width after passing through both of the lenses. For recollimation to occur, the lenses must be placed a distance apart equal to the sum of their focal lengths, 240mm in this case. If arranged in this configuration, the lenses form what is known as a beam expander. Once again, the positioning

of these lenses is of utmost importance to ensure that the shape of the wavefront returns to collimated, so each one was mounted in a tip/tilt mount. L3 was additionally mounted on a linear translation stage so that the positioning could be carefully adjusted to achieve proper recollimation. The factor of magnification that is achieved by the lens pair can easily be found using a ratio of their focal lengths. In this case, the beam is magnified by a factor of 1/5. In the original design, no beam expanders were included, as we did not realize how small the aperture of the Faraday Rotator (FR) was for our setup. Because the FR only had an aperture of 2mm in diameter, this beam expander was introduced such that the beam would have a diameter under 2mm, to maximize the amount of light that could be captured in the cavity. To check the collimation of the light after the beam expander, a Shack-Hartmann Wavefront sensor was used, as the beam diameter was now too small to allow for any useful information to be gleaned from the use of a shear plate. Using the Shack-Hartmann, we measured that the radius of curvature of the wavefront at this point was 104.9 m, which is the largest that I could adjust it to be and therefore had the highest degree of collimation that we could manage.

Following the beam expander lenses, component P, an optical polarizer, was added to the system. The alignment of this component was relatively simple, as it does not alter the direction or shape of the wavefront of the beam upon the light's passage through it. Despite this, it is still good practice to use the back-reflection of the light incident on the polarizer to judge how close to normal incidence the light is on the polarizer. The polarizer is mounted inside a rotation mount, so it was then properly rotated to maximize the amount of light allowed to pass through it. Due to the power of the laser, it was difficult to determine the exact point of maximum throughput. An alternate method to determining the maximum power passed through the system is to find the point where the power is at its minimum and then rotate the polarizer 90° from that point.

The following component was added to introduce a level of redundancy beyond what we had originally planned. Component GTP is a Glan-Thompson polarizer, which does a better job than the first polarizer at eliminating unwanted polarizations of light. This component is also mounted in a rotation mount, so the same procedure was used to ensure that the maximum amount of light was passing through it. After passing through the GTP, there were several trailing dots of light aside from the brightest one, which is the only one that we wanted to progress through the system, so another aperture was introduced immediately after the GTP in the form of the component AP2 to block this unwanted light from proceeding further into the system.

After both of the polarizers, we have very linearly polarized light, but it is not polarized vertically, to maximize the amount of light that passes through the polarizing beam-splitter (PBS), so a half-wave plate (HWP) was introduced before the PBS. Both the HWP and PBS were installed at the same time so that they could be used to check that the maximum amount of light is passing into the back half of the system. The HWP is mounted in a rotation mount, so after both are aligned, the HWP is rotated until the maximum amount of light passes through the PBS. Alternatively, the point at which a minimum amount of light passes through the PBS can be determined, and the HWP can be rotated 45° from that point to reach the point of maximum transmission. There is but another method to check in this case, as any light not transmitted through the PBS is reflected out of the system at a 45° angle and can be captured on a screen. The point at which the light captured on the screen is minimized indicates that you are properly aligned and the most amount of light possible is passing through the PBS. Because the screen is capturing stray light that points toward anyone who may be working in the lab, it is safest to keep this blocked by the screen.

Following the PBS is one of our most critical components, the Faraday rotator, FR. In this case, we have installed a 45° FR. Due to polarization rotation through an optically active material

always occurring in the same direction of the light through the material, this allows any light reflected back on itself after the FR to exit through the other side of the PBS than the screen since it has undergone a 90° rotation in polarization due to two passes through the FR. The direction of the FR is not important due to it having a set rotation of 45° , but it still was mounted in a rotation mount to allow for any additional rotational adjustment just in case there was a defect for some reason and the rotation of the FR made a difference in the amount of light passed.

Without a good way to determine the alignment of the optical cavity quantitatively, we had to depend on qualitative assessments of alignment, and as that requires an ability to visibly see the size of the spot created by the beam, another beam expander had to be introduced with L4 and L5. L4 is a 50mm focal length lens mounted in a tip/tilt mount, and L5 is a 300mm focal length lens mounted in a tip/tilt mount on a two-axis translation stage. The combination of these two lenses made the beam expand by a factor of 6. These two had to be placed a distance of 350mm apart to achieve recollimation, which was once again determined using the Shack-Hartmann wavefront sensor. The wavefront was measured to have a radius of curvature of 31.9m at this point, which was the largest that the wavefront curvature could be managed. From here, the recollimated beam passes through L6, a 250mm lens, which we often refer to as our mode-matching lens. This lens has always been a part of our design, as it allows the curvature of the wavefront to match the curvature of our second mirror when properly aligned. Without this lens, our resonant cavity would not be possible.

The last two components, M3 and M4, are the most important in this entire design. These are the two mirrors used to construct of the resonant cavity. M3 is an 80% reflective partial mirror designed for use with the 532nm wavelength. Because it is transmissive to most other wavelengths, the mirror appears greenish in Fig. 6. M3 is mounted on a linear translation stage and a motor-

controlled rotation stage while also being in a tip-tilt mount. M4 is the only curved mirror in this system. The curved side of the mirror has a radius of curvature of 500mm, and thus, the mirror has a focal length of 250mm. This mirror is mounted in a tip/tilt mount on top of a motorized linear translation stage, a manual linear translation stage arranged perpendicular to the other, and a motorized rotation stage. Both of the rotation stages needed to use custom-made adapter components to function with this setup. These components were created using 3-D printing and heat-set threading. Additional care was taken with the motorized linear translation stage. Its linear actuator must have fine enough adjustments to accommodate necessary changes in cavity length due to sample insertion. The linear actuator changes position by a unit called a microstep, and in the case of this actuator, the microstep is $0.047625\mu\text{m}$. Not only is this much smaller than the estimated 0.5mm of required movement disclosed in the background section, it should allow for much finer control than would be acquired with a manually controlled translation stage.

Though M3 is an 80% mirror, which means that 80% of the light will never make it into the cavity, the Helmholtz coil is only around the interior of the cavity. Because we can modulate the current to the coil, we can make it so that the only light that is modulating is that which enters the cavity. Thus, even though much of the light never enters the cavity, we can use the non-reciprocal Faraday rotation in the sample to create modulation in the polarization, and thus a modulated output. This means we can use a lock-in amplifier on our detector and focus exclusively on the modulating portion, thus significantly shrinking our SNR despite the fact that most of the light never enters the cavity.

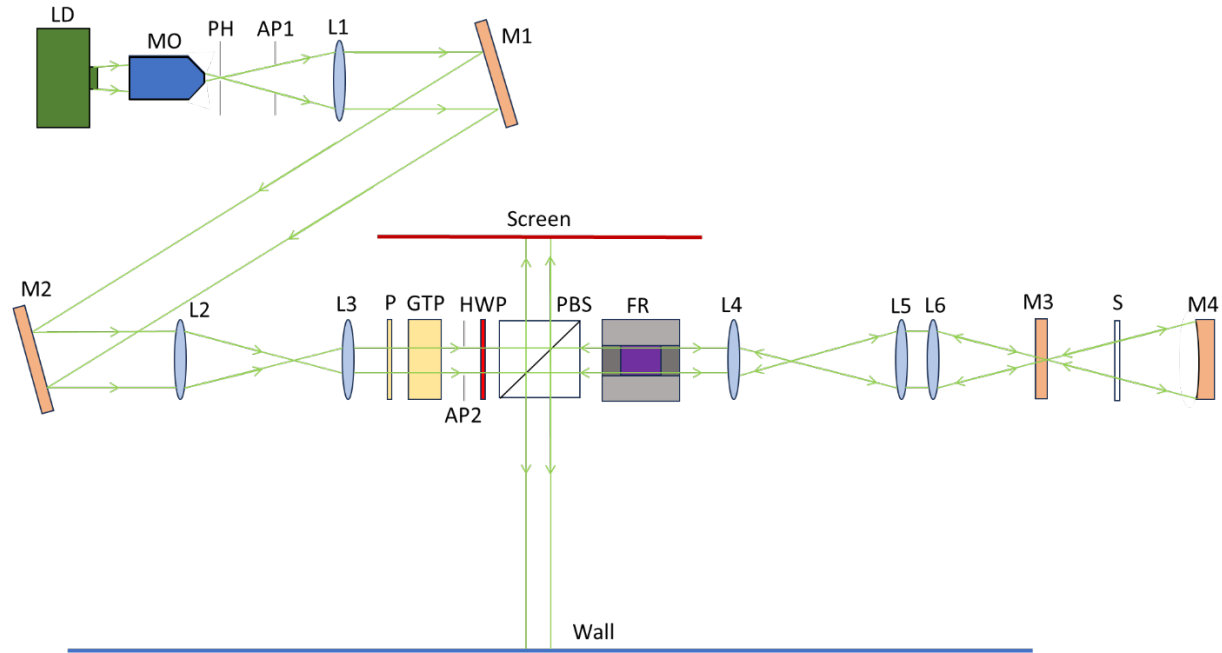


Figure 8: Schematic Depiction of Autocollimation Setup

For proper system alignment, M3 has to be placed at the minimum spot of the converging beam after the mode-matching lens, L6. M4 then needs to be placed 500mm behind M3. Because the output of the cavity is along the same path as the input to the cavity, it is difficult to check for proper alignment of the mirrors. To perform a qualitative alignment of a resonant optical cavity, the beam exiting the system after traveling through the cavity must be allowed to propagate a distance and then be captured on a screen. In the case of this experiment, the beam was allowed to propagate several meters onto the wall behind the table with the setup, as seen in Fig. 8. Interestingly, the FR created a visible back-reflection that was captured by the PBS and sent out along the desired detection direction, where the back-reflected beam would travel. For the cavity to be properly aligned, it is required that the returning beam be recollimated. If properly recollimated, the resulting spot on the wall would be comparable with that of the back-reflection from the FR, which was measured and confirmed to be collimated.

To achieve the proper placement of the partial mirror, M3, one has a couple of qualitative measurements they can use. To begin, the spot on the inner (in reference to the cavity) surface of the mirror from L6 must be at its minimum diameter. Though this is hard to determine, this qualitative measure can be used to get close to the correct placement of the mirror. When you are close to the proper placement, it is important to put a small screen in the cavity to block the light from the second mirror, thus minimizing the number of factors that could change what travels back through the system. A glow should be seen on the wall alongside a small dot. The glow should match the size and shape of the spot that is back-reflected off of the FR. When these match in size, any spots that are visible on other components (lenses) should be aligned so that they overlap as much as possible using the tip/tilt of the mirror, and then the spot on the wall should be checked that it still matches the size of the back-reflection. This can be iteratively done until satisfied. For additional accuracy, the path length of the light exiting the system can be extended before it reaches the wall by using flat mirrors to fold the beam from one mirror to another and thus increase the total length traveled by the light exiting the system.

For mirror M4, a similar method can be used to achieve proper alignment. The first thing that should be done is to ensure the mirror is placed in approximately the correct spot using a meterstick or ruler. Once M4 is nearly at the correct distance away from M3, the position of M4 should be adjusted until the spot from the light that passed through M3 is centered on the mirror. If the light cannot be seen, putting a thin, translucent material just in front of the lens may allow you to see the positioning of both the spot of the light and the mirror. The cavity should be empty for the next step of the alignment process, as the light must be allowed to travel back upon the path it took to enter the cavity. Rather than trying to overlap the spot on the wall from M4 with the spot from M3, make sure that M4 sends a spot that is slightly offset from the M3 spot position. The

distance between the mirrors is then adjusted using the motorized translation stage until all of the spots that appear on the wall are the same size. The spot that was just made from a reflection off of M4 must then be adjusted until it overlaps with the spot made from the reflection off of M3. Upon making sure that all of these qualitative measures are achieved as best as possible, the cavity was very close to proper resonant cavity alignment. Still, as there has not been a quantitative test of the quality of cavity alignment, it is nigh impossible to say that it is perfectly aligned.

Though all of the system pictured in Fig. 6 has been described, there are a few components in Fig. 7 that have not been touched on. The component labeled PD is a photodetector, and the component labeled S is the sample inserted into the cavity. The eventual goal of this setup is to allow for measurements of Faraday rotation introduced by a sample in the cavity using a simple photodetector or power meter. For this to be possible, a Helmholtz coil is put around the cavity so that a controlled magnetic field can be introduced on the sample, causing Faraday rotation.

5. RESULTS

To check whether or not the cavity was aligned properly, several different optical power measurements were taken at different points along the length of the setup. Those measurements will be described in this section, and their implications will be discussed next. All positions of the measurements will be described using Fig. 7 and appropriate supplemental figures are shown in this section as a reference. The measurements were all taken in one sitting with the current to the LD set as 200mA, which is a lower current level than is listed as typical for this laser, to keep it at a safer level.

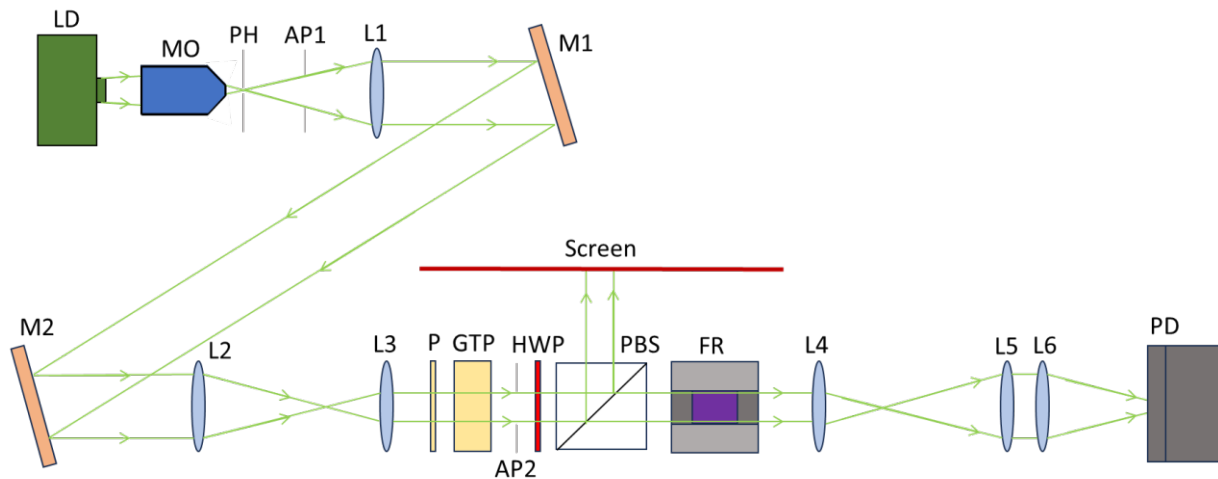


Figure 9: Schematic Configuration for Measurement of Light Incident on the Partial Mirror

The first measurement was taken between L6 and M3, and the appropriate configuration can be seen in Fig. 9. This measures the light incident on the partial mirror, $83.25\mu\text{W}$.

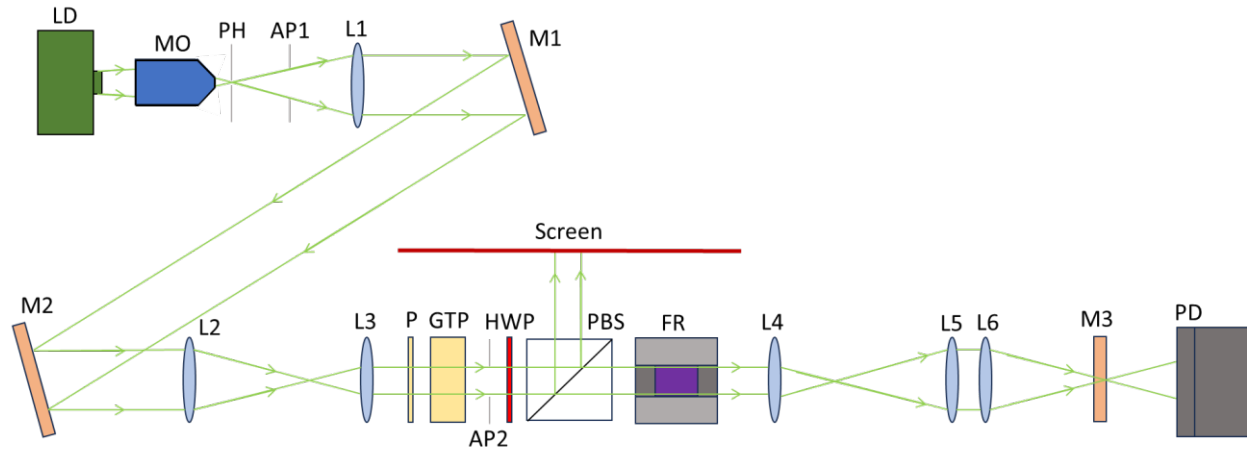


Figure 10: Schematic Configuration for Measurement of Light Entering the Cavity

The second measurement of interest is between M3 and M4, which can be visualized as seen in Fig. 10. This is a measurement of the amount of light allowed to enter the cavity. Two values were taken for this measurement. One was taken when the photodetector face was parallel to the mirror M3, and the second was taken when the photodetector was tilted slightly to remove the influence of any light that was reflecting off the photodetector to the mirror, and back to the detector. The first value (including back-reflection) was $19.04\mu\text{W}$, and the second (without back-reflection) was $17.37\mu\text{W}$.

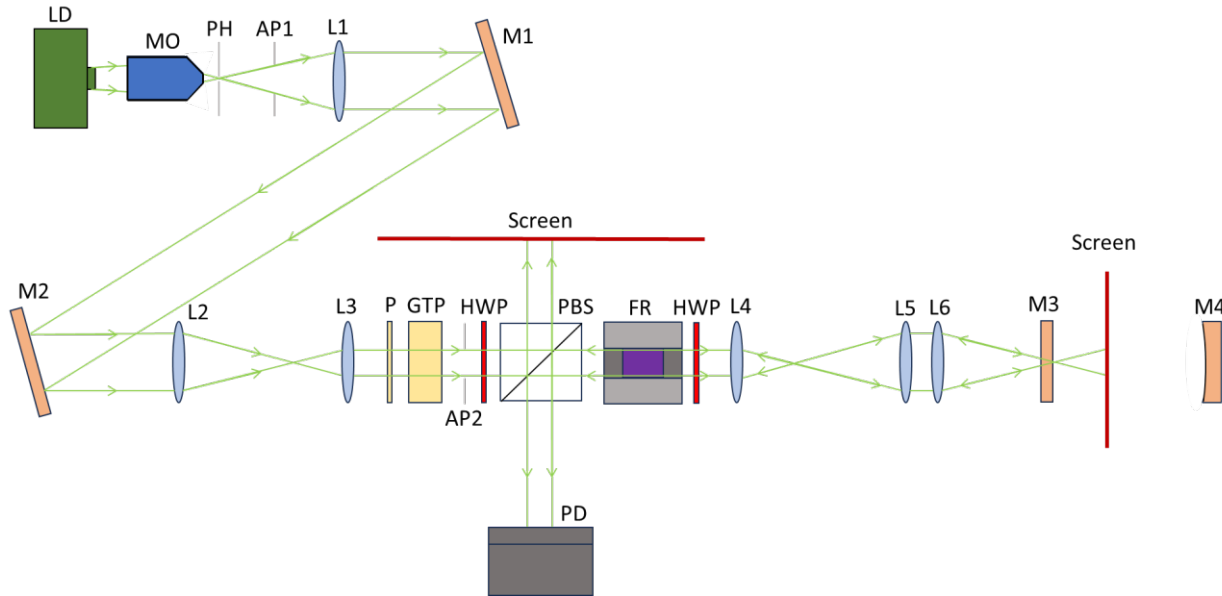


Figure 11: Schematic Configuration for Measurement of Light in a Non-Resonating System

The next measurement was that of the system's output as normally shown, with the photodetector in the position of PD, but M4 blocked by a screen, so there is no resonance, as seen in Fig. 11. This value was $31.03\mu\text{W}$.

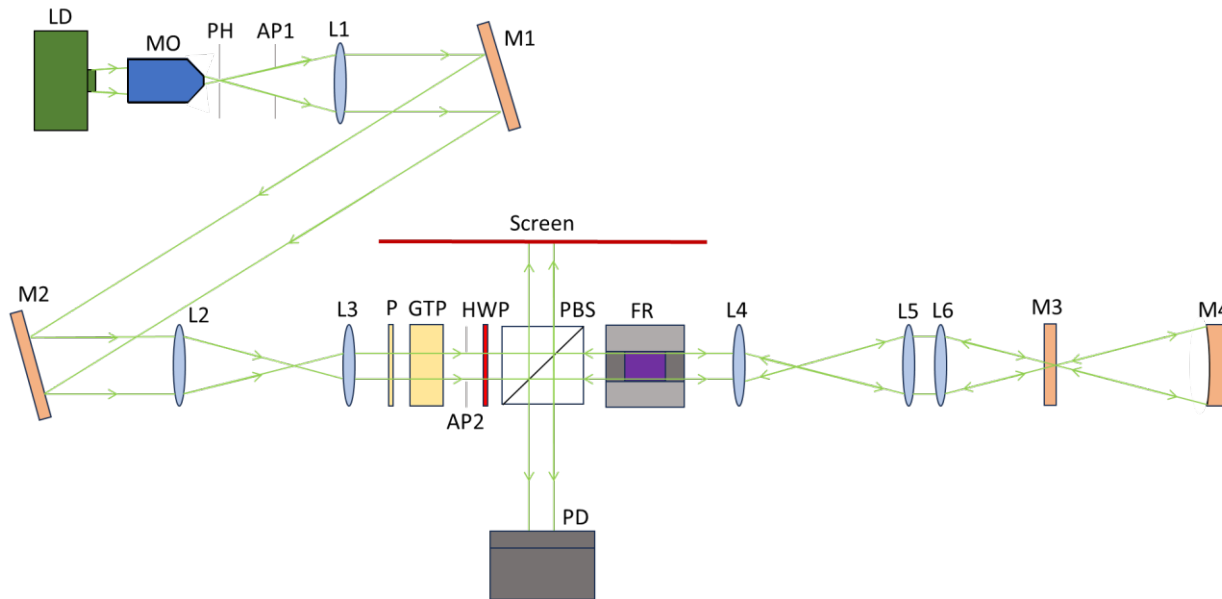


Figure 12: Schematic Configuration for the Measurement of Light in a Resonating System

The final measurement to be taken is the system's output without the screen in the way of M4, so the output of the system with resonance included, as can be seen in Fig. 12. This value was $38.70\mu\text{W}$. When the values of the output with and without the mirror M4 are compared, the ratio is found to be $31.03\mu\text{W}/38.70\mu\text{W} = 80.2\%$.

6. DISCUSSION

Based on the two key measurements of the total output of the system with and without the addition of mirror M4 (see Fig. 11 and Fig. 12), it would appear that we have either achieved resonance or come very close to achieving it. Despite this seeming success, there is a significant discrepancy between the power measured as incident on M3 and the output power of the whole system, which should be comparable to that incident power. The optical power before and after each component after the polarizing beam splitter was then measured, and the Faraday rotator introduced the most loss, with a difference of $0.65\mu\text{W}$ between the measurements before and after. Thus, none of the components seemed to account for the surprising loss of more than 50% of our light.

In our analysis of this issue, we determined that the most likely cause was deconstructive interference in the cavity, as the FSR of the cavity is much smaller than the bandwidth of the input laser; thus a little over half of the light will destructively interfere inside the cavity and not contribute to overall power measurements of the output.

In a perfectly aligned and lossless system, the power that is detected at the output of the system should be equivalent to the power that is input to the system. With the blockage of the mirror M4 (see Fig. 11), the output power should be measured as 80% of the input power. Because of the fact that this relationship holds up for the experimental values with and without the presence of mirror M4 in the calculation, we can conclude that the cavity is indeed properly aligned and resonating in our optical setup.

The physical optical resonator setup achieved resonance, which is the most important part of this study. This indicates that future research can also be done with this setup.

7. LIMITATIONS

When working on this project, there were several limitations to what we could do. One of the foremost limitations was budget. We did receive a research grant to purchase some materials for this project. Still, based on our budget, we needed to operate by mostly using optical components that were available through the school or specific professors. Due to this limitation, it sometimes took a while to gather the appropriate optical and optomechanical components to construct this setup. Because we were using many components that belonged to others and were used previously in other setups, not all of them were well-marked with their optical quality or surface quality.

Another limitation that we ran into has to do with the motorized linear actuator that we were using with the curved mirror, M4 (see Fig. 6 and Fig. 7). This device is designed to be connected to a computer, but when we sought to connect it to our computer, the cable that was used was inappropriate for the application. Instead of using what we already had, we needed to get a new cable to connect it so that none of the leads were swapped and communication with the device would be possible. After getting the correct hardware to fit with the discontinued linear actuator, we had to make sure that we revised the command format that was used to communicate with the linear actuator, as the default communication language was too new for use with the device that we were able to get our hands on.

In the course of this project, a qualitative method to check the quality of the resonant optical cavity was not determined with enough confidence and understanding to implement it before this

thesis was completed. Therefore, we are unable to perform checks on additional information about the cavity, such as its Q-factor and finesse. As such, we are limited in our capacity to give any additional information regarding the quality of the cavity that has been constructed. A major part of this limitation is that the output and input beams to the resonant cavity are overlapping and tracing the same path. Due to this, any components that are added into the path in hopes of measuring the output directly after the cavity would only succeed in blocking the light going into the cavity and thus not give any information about the cavity.

8. CONCLUSIONS

Based on all of the information that can be gleaned from the measurements we took, it seems that a resonant optical cavity has indeed been constructed and properly aligned. Though we cannot compute any information about the resonant cavity and its quality of alignment, such as Q-factor and finesse, from the measurements that we can acquire it seems that the cavity is either properly aligned or very nearly so, as the output of the system with mirror M4 blocked is about 80% of the output when M4 is uncovered, and the cavity is allowed to resonate. This would not be the case if the cavity was not resonating, and the percentage would be significantly greater than 80%.

Despite the ability to reach this conclusion, we have not placed a sample into the resonant cavity yet and made sure that it can still resonate. While our current data give us enough information to know that we have achieved proper alignment and resonance in the optical cavity, we have not done enough testing with samples inside the cavity to be able to confirm that it works well for its intended future purpose.

9. FUTURE WORK

There is much future work to be done with this project. The most important future work is regarding the insertion of a sample into the cavity. First and foremost, it should be checked that the cavity can be adjusted to still resonate with an additional component added to it. This can be done using the same methodology described earlier in this document. From there, measurements using the Helmholtz coil can commence to measure the Faraday rotation introduced from the optical activity of a thin-film sample. For these measurements, it is wise to introduce mechanical components for the controlled movement of the sample to conduct a Raster scan for imaging the magneto-optical response of the sample by making the light incident on different sections of it.

Beyond these future investigations, it may be useful to investigate possible avenues to evaluate an optical resonant cavity that uses the same component as an input and output, making the output beam overlap with the input. Though this is a difficult issue, solving this issue may provide avenues by which to conduct other experiments in the future with optical systems that reflect upon themselves. Concerning this, it may be useful to use a scanning Fabry-Perot etalon outside of the system to evaluate the finesse of the cavity. Another known method to characterize the cavity with high precision is using the cavity ring-down technique to validate the characterizations conducted in the current work (Galzerano, Suerra and Gianotti).

In future investigations, it may be important to consider the impact of the magneto-optic Kerr effect, which also serves to change the angle of polarization of light upon reflection from the surface of samples, as it may impact the values that are measured through the system.

LIST OF REFERENCES

- Faraday, Michael. "V. Experimental researches in electricity." *Philosophical Transactions of the Royal Society of London* 122 (1832): 125-162.
<<https://royalsocietypublishing.org/doi/abs/10.1098/rstl.1832.0006>>.
- Galzerano, Gianluca, et al. "Accurate measurement of optical resonator finesse." *IEEE Transactions on Instrumentation and Measurement* 69.11 (2020): 9119-9123.
- Gianella, Michele, et al. "Sensitive detection of HO₂ radicals produced in an atmospheric pressure plasma using Faraday rotation cavity ring-down spectroscopy." *The Journal of Chemical Physics* 151.124202 (2019). PDF.
- Jo, Jae Young, et al. "Sensitive measurement of the magneto-optic effect in the near infrared wavelength region with weak alternating magnetic fields." *Optical Materials Express* 8.9 (2018): 2636-2642. PDF.
- Kogelnik, Herwig and Tingye Li. "Laser Beams and Resonators." *Applied Optics* 5.10 (1966): 1550-1567. PDF.
- Peatross, Justin and Michael Ware. "Physics of Light and Optics." Available at optics.byu.edu, 2015. 98-104.
- Reza, Syed Azer, Maarij Syed and Cody Brelage. "Resonant Cavity Design for Enhanced Magneto Optic Measurements." *SPIE Optics & Photonics*. San Diego, California: n.p., n.d.

Svelto, Orazio. "Principles of Lasers." New York: Springer, 2010. 131-171.

Syed, Maarij, et al. "Use of AC Faraday rotation as a complementary technique in material characterization." *AIP Advances* 9.125242 (2019). PDF.

Valev, V. K., J. Wouters and T. Verbiest. "Precise measurements of Faraday rotation using ac magnetic fields." *American Journal of Physics* 76.7 (2008): 626-629.

Van Baak, D. A. "Resonant Faraday rotation as a probe of atomic dispersion." *American Journal of Physics* (1996): 724-725.

Yariv, Amnon and Pochi Yeh. "Photonics: Optical Electronics in Modern Communications." Yariv, Amnon and Pochi Yeh. *Photonics: optical electronics in modern communications*. Oxford University Press, 2007. 110-147.